

Attosecond time-resolved photoelectron spectroscopy of surfaces

Uwe Thumm and Chang-hua Zhang

Department of Physics, Kansas State University, Manhattan, Kansas 66506, USA

Abstract. We discuss streaking time delays for photoemission from solid model surfaces as a function of the degree of the initial-wave-function localization and including the dynamical plasmon response to the motion of the photoelectron.

Keywords: Photoemission, Streaking, Plasmon, Time delay, Attosecond, Spectroscopy

PACS: 32.30.-r, 73.20.Mf, 78.47.J-, 78.56.-a

INTRODUCTION

Due to significant progress in laser technology, sub-femtosecond extreme ultraviolet (XUV) pulses can be generated and synchronized with a delayed infrared (IR) laser pulse. Photoelectron emission by ultrashort XUV pulses into the field of an IR pulse allows the recording of XUV-IR-delay dependent (or “streaked”) photoemission spectra that show periodic shifts in measured photoelectron energies. These energies oscillate with the IR carrier frequency and can be converted into apparent time delays. By comparing oscillating streaking traces that are due to photoemission from different initial electronic states, *relative* delays can be resolved at the intrinsic time scale of the electronic motion in matter. This has enabled the time-resolved observation of the electron dynamics in atoms [1-3] and solids [4]. It promises unprecedented sensitive experimental tests of the collective electron dynamics in solids and novel plasmonic devices [5-8].

The interpretation of these sub-fs temporal shifts in streaked spectra is still a matter of debate. For atomic targets, this debate revolves around the importance of contributions to the photoemission time delay due to short- and long-ranged interactions of the photoelectron with the residual ion [9-11] and the IR-laser field [10-13] and due to many-electron effects [3,12]. For solid targets, the detailed interpretation of relative streaking time delays is further complicated by their complex electronic band structure [4,14], elastic and inelastic scattering of the released photoelectron in the solid [15-17], the excitation of surface and bulk plasmon modes [18], and the need for estimating the skin depths of the streaking IR-laser field [17,18].

CALCULATION OF STREAKING TIME DELAYS

The basic theory is best outlined by assuming photoelectron emission in direction perpendicular to the surface and by modeling the solid as a slab with N atomic core layers. For simplicity, we further assume a one dimensional solid and represent each

atomic core by an effective Gaussian potential [19]. Occupied initial states of the slab can then be obtained by numerically solving the Schrödinger equation (SE)

$$\varepsilon_n \psi_n(z) = \left[-\frac{1}{2} \frac{d^2}{dz^2} + V(z) \right] \psi_n(z), \quad V(z) = V_0 - \frac{B_0}{\sigma} \sum_{i=1}^N \exp \left\{ -\frac{[z + (i + 0.5a_{latt})]^2}{2\sigma^2} \right\}. \quad (1)$$

Unless specified otherwise, we use atomic units throughout this paper. The parameter σ controls the overlap between adjacent core potentials. a_{latt} is the lattice spacing. V_0 and B_0 are adjusted so that the most important characteristics of metal valence band (work function and band widths) are approximately reproduced.

Next, the time-dependent SE

$$i \frac{d}{dt} \psi_n(z, t) = \left\{ -\frac{1}{2} \left[i \frac{d}{dz} + A_L(t - \Delta t) \right]^2 + V(z) \right\} \psi_n(z, t), \quad \psi_n(z, 0) = \psi_n(z), \quad (2)$$

is solved by numerical propagation [12] of each occupied initial state in the oscillating field of the streaking IR laser with frequency $\omega_L = 2\pi/T_L$ and vector potential

$$A_L(t) = A_0 \sin^2 \left(\frac{\pi t}{T_L} \right) \cos \left(\omega_L t - \frac{T_L}{2} \right) \left[\exp \left(\frac{z}{\delta_L} \right) \Theta(-z) + \Theta(z) \right]. \quad (3)$$

The bulk is confined to the region $z < 0$. δ_L is the IR skin depth. For the delay between the centers of the XUV and IR pulses, we use the convention that $\Delta t > 0$ corresponds to the XUV preceding the IR pulse. We calculate the photoelectron wave packet $\delta\psi_n(z, t)$ that is emitted from the initially occupied laser-dressed wave function $\psi_n(z, t)$ by numerically propagation the inhomogeneous SE

$$i \frac{d}{dt} \delta\psi_n(z, t) = \left[-\frac{1}{2} \left[i \frac{d}{dz} + A_L(t - \Delta t) \right]^2 + V(z) + i\Sigma_{ph}(z) \right] \delta\psi_n(z, t) + z E_X(t) \psi_n(z, t), \quad (4)$$

for a Gaussian XUV pulse with frequency $\omega_X = 2\pi/T_X$ and electric-field strength,

$$E_X(t) \sim \exp \left[-2 \ln 2 \left(\frac{t}{T_X} \right)^2 \right] \sin(\omega_X t). \quad (5)$$

Scattering of the released photoelectron inside the solid is approximated by the phenomenological potential $\Sigma_{ph}(z) = -\sqrt{2E_{kin}} \Theta(-z)/(2\lambda)$ in terms of the electron mean-free path λ and center of energy (COE) of the photoelectron wave packet E_{kin} .

After solving Eq. 4 for a given delay Δt , the Fourier transforms $\delta\phi_n(k, \Delta t)$ of $\delta\psi_n(z, t \rightarrow \infty)$ yield the probability and COE for photoemission from $\psi_n(z)$,

$$P_n(\Delta t) = \int dk |\delta\phi(k, \Delta t)|^2, \quad E_{COE,n}(\Delta t) = \frac{1}{2P_n(\Delta t)} \int dk k |\delta\phi(k, \Delta t)|^2, \quad (6)$$

respectively. The streaking delay τ_s is obtained by fitting the parameters α , β , and τ_s in the band-averaged COE

$$E_{COE}(\Delta t) = \frac{1}{\sum_{occ} P_n(\Delta t)} \sum_{occ} P_n(\Delta t) E_{COE,n}(\Delta t) = \alpha + \beta A_L(\Delta t - \tau_s) \quad (7)$$

over a range (e.g., $-T_L/2 \leq \Delta t \leq T_L/2$) of XUV-IR pulse delays.

Dependence on the localization of the initial-state wave function

As a numerical example, we discuss results for band-averaged photoemission delays τ_S as a function of σ for a slab with $N = 47$ rows and lattice spacing $a_{\text{latt}} = 6$. We take an IR laser pulse with 5×10^{11} W/cm² peak intensity, 800 nm wavelength, and $T_L = 8$ fs duration. The XUV pulse has a length of 300 as. If sufficiently small to validate Eq. 4, its intensity is irrelevant for the computation of τ_S . The streaking delays in Fig. 1 show a bimodal behavior, with a fast decrease with decreasing wave-function localization near $\sigma/a_{\text{latt}} = 0.3$, and become insensitive to the changes in λ for photoemission from (mostly) delocalized states with $\sigma/a_{\text{latt}} > 0.4$.

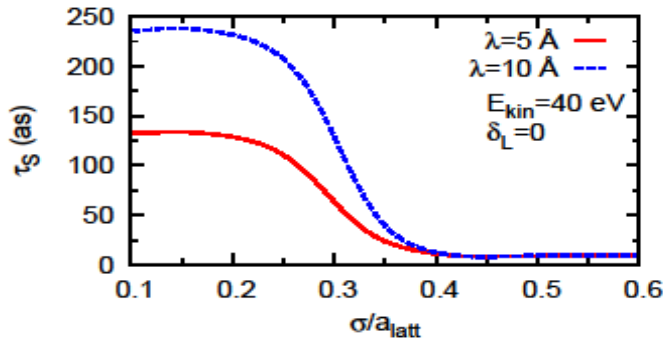


FIGURE 1 (Color online) Streaking delay in units of attoseconds as a function of the wave-function-localization parameter σ in units of the lattice spacing a_{latt} for two photoelectron mean-free paths λ and an average photoelectron kinetic energy of 40 eV.

The dependence of τ_S on the photoelectron energy E_{kin} (i.e., on $\hbar\omega_X$) is shown in Fig. 2. For emission from localized initial states ($\sigma/a_{\text{latt}} = 0.1$), τ_S can be understood as the average time $\lambda/\sqrt{2E_{\text{kin}}}$ needed for released photoelectrons to travel an average distance λ inside the solid with velocity $\sqrt{2E_{\text{kin}}}$. Indeed, τ_S and $\lambda/\langle v \rangle = \lambda/\sqrt{2E_{\text{kin}}}$ cannot be distinguished in Fig. 2. However, this interpretation starts to break down for increasing σ/a_{latt} , i.e., for increasingly delocalized initial states, and quickly becomes invalid for larger σ/a_{latt} . For photoemission from a fully delocalized initial state with $\sigma/a_{\text{latt}} = 0.5$, τ_S decreases very slowly as a function of E_{kin} and strongly deviates from $\lambda/\langle v \rangle$ over the entire displayed range of kinetic energies.

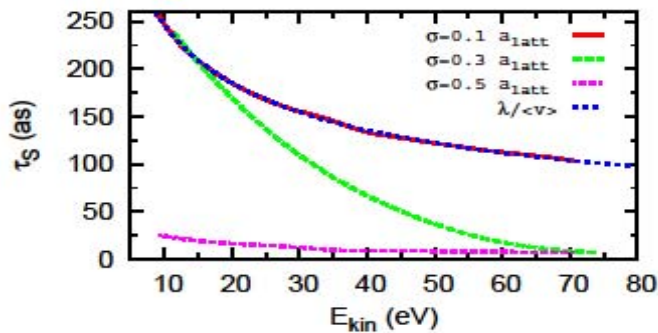


FIGURE 2 (Color online) Streaking delay as a function of the photoelectron kinetic energy for different wave-function-localization parameters σ in units of the lattice spacing a_{latt} for $\lambda = 5 \text{ \AA}$ and vanishing IR skin depth.

The bimodal behavior of the streaking time delay as a function of the localization parameter σ agrees with the main finding of the streaking experiments in Ref. [4], where photoelectrons from core and conduction band levels of tungsten were released by 91 eV XUV photons and measured with energies near 55 and 81 eV, respectively. If we assign (without further justification of the precise numerical value)

the localization parameter $\sigma/a_{\text{latt}}=0.1$ to the localized $4f$ core levels of tungsten and any value $\sigma/a_{\text{latt}} \geq 0.3$ to the delocalized conduction band levels, a relative streaking time delay 120 as can be deduced from Fig. 2, in accord with the originally published measured value of 110 ± 70 as [4,17,19]. Figure 2 suggests that future experiments would have to use smaller XUV photon energies, resulting in $E_{kin} < 60$ eV, in order to probe the localization properties of the initial-state wave functions.

Probing plasmon-response effects in streaked photoelectron spectra

The release of conduction-band electrons from a metal surface by a sub-femtosecond XUV pulse and their propagation through and near the solid provoke a dielectric response in the solid that acts back on the electron wave packet [4,18]. For the purpose of modeling this many-electron response only, we assume the photoelectron moves as a classical particle at constant speed $v_z = \sqrt{2E_{kin}} = \sqrt{2(\omega_X - |\varepsilon_n|)}$ in direction perpendicular to the surface, corresponding to the charge density $\rho(\mathbf{r}, t) = \delta(\mathbf{r}_{\parallel})\delta(z - v_z t)$. The response of the solid is described by the complex self interaction potential

$$\Sigma(z, v_z) = \Sigma_r(z, v_z) + i\Sigma_i(z, v_z), \quad (8)$$

which converges for large distances from the surface to the classical image potential $-1/(4z)$. Its real part Σ_r models virtual excitations of bulk and surface plasmons and electron-hole pairs in the solid, while its imaginary part Σ_i accounts for a net energy transfer between the photoelectron and collective modes of the substrate. We model the undistorted solid as a wide slab in jellium approximation [20] by replacing the potential $V(z)$ in Eqs. 1 and 2 with $V_j(z) + \Sigma_r(z, 0)$, where $V_j(z) = -V_0/\{1 + \exp(z/a)\}$ is a smeared-out step potential of width γ at both sides of the solid-vacuum interface. The effect of the dielectric response on the released photoelectron wave packet is accounted for by replacing $V(z) + i\Sigma_{ph}(z, v_z)$ in Eq. 3 with $V_j(z) + \Sigma(z, v_z)$.

We calculate $\Sigma(z, v_z)$ based on phenomenological dielectric functions $\varepsilon_B(\mathbf{k}, \omega)$ and $\varepsilon_S(\mathbf{k}, \omega)$ that model plasmon and particle-hole excitations by the photoelectron in the bulk and at the surface [21]. The calculation proceeds analytically by propagating the initial (vacuum) state of the bulk and surface plasmon quantum field $\Psi(t=0)$, subject to the interaction $H_{int} = \int d\mathbf{r} \rho(\mathbf{r}, t)\Psi(\mathbf{r}, t = 0)$ [22]. It results in a lengthy expression for $\Sigma(t, v_z) = \frac{1}{2} \langle \Psi(t) | H_{int}(t) | \Psi(t) \rangle$ that depends on the bulk (ω_B) and surface plasmon frequency ($\omega_S = \omega_B/\sqrt{2}$) and can be evaluated numerically [18].

Figure 3 shows streaked photoemission spectra for an aluminum model surface with $V_0 = 10.2$ eV, $\omega_S = 0.378$, $\gamma = 1.4$ Å, $\lambda = 5$ Å, and $\delta_L = 0$, and for a 300 as XUV pulse centered at $\hbar\omega_X = 40$ eV. The streaked spectrum in Fig. 3a is obtained by replacing Σ_i in Eq. 8 with Σ_{ph} while keeping fully “dynamical” real part Σ_r . As a reference, we calculate the spectrum in Fig. 3b using the “static” response obtained by replacing $\Sigma(z, v_z)$ with $\Sigma_r(z, 0) + i\Sigma_{ph}(z, v_z)$. The COEs for these two spectra are shifted by the streaking-time-delay difference $\Delta\tau_{\text{wake}} = \tau_{S, dyn} - \tau_{S, sta} = 100$ as (Fig. 3c).

Streaking delay differences $\Delta\tau_{\text{wake}}$ are shown for different mean-free paths in Fig. 4a and for different plasmon frequencies (i.e., electron densities) in Fig. 4b as a function of $\hbar\omega_X$. In Fig. 4a we use $\omega_S = 0.378$, in Fig. 4b $\lambda = 5 \text{ \AA}$. All other parameters are as in Fig. 3. Increasing λ by a factor of two significantly increases $\Delta\tau_{\text{wake}}$ for $\hbar\omega_X < 50 \text{ eV}$, but has little influence at larger ω_X (Fig. 4a). We find that, in general, $\Delta\tau_{\text{wake}}(2\lambda) \neq \Delta\tau_{\text{wake}}(\lambda)$, which is incompatible with the interpretation [4,16] of the observed [4] delay between photoemission from core and conduction-band levels in tungsten in terms of the photoelectron's travel time in the solid, $\lambda/\langle v \rangle$. Decreasing ω_S shifts the double-hump structure to lower ω_X (lower E_{kin}), as expected in view of the decreased thresholds for plasmon excitations (Fig. 4b).

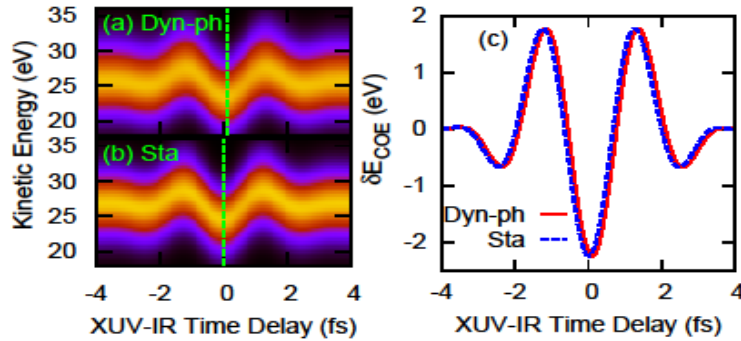


FIGURE 3 (Color online) Streaked photoelectron spectra as a function of the pump-probe delay Δt for a model aluminum surface and $\hbar\omega_X = 40 \text{ eV}$: (a) including the dynamical plasmon response *during* the motion of the photoelectron; (b) including the plasmon response in static (adiabatic) approximation, allowing the plasmon field an infinite time to adjust to the perturbation by a classical photoelectron at any given position. (c) Centers of energy of the spectra in (a) and (b) showing a streaking-time-delay difference $\Delta\tau_{\text{wake}} = 100 \text{ as}$.

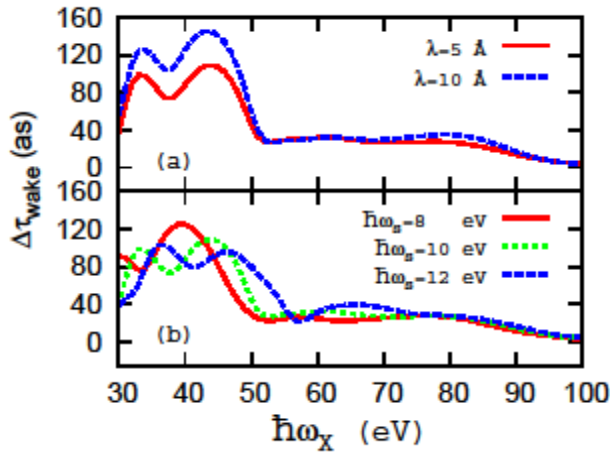


FIGURE 4 (Color online) Streaking-delay difference $\Delta\tau_{\text{wake}}$, induced by the non-adiabatic response of model substrates, as a function of the XUV photon energy for different (a) electron mean-free paths λ and (b) surface plasmon frequencies ω_S .

CONCLUSIONS

Streaking delays in photoemission spectra from metal surfaces depend on the degree of localization of the initial-state wave functions and feature a characteristic bimodal behavior. Numerical results for a simple model surface indicate that electron emission from localized (delocalized) initial states leads to large (small) streaking delays. This confirms previous mechanisms and interpretations [12,17] for the

accumulation (or lack thereof) of quantum mechanical phase during the interaction of photoelectrons that originate in core and conduction band levels, in qualitative agreement with experiments [4].

The release and propagation of photoelectrons triggers a dynamical dielectric response in the substrate that we model in term of the excitation of bulk and surface plasmons (and electron-hole pairs) *during* the motion of the photoelectron [18]. The influence of this dynamical response on the streaking delay sensitively depends on the XUV photon frequency and characteristics of the substrate, such as the bulk- and surface-plasmon frequency, the IR skin depth, and (in)elastic electron-scattering cross sections. The measurement of streaked electron spectra may thus be applied to probe the ultra-fast plasmonic response of solids to external perturbations with unprecedented accuracy, at the scale of attoseconds. Our model calculations predict streaking-delay contributions, due to the non-adiabatic plasmon response, of more than 50 as that can be resolved with contemporary laser technology [3].

ACKNOWLEDGMENTS

This work was supported by the NSF and the Division of Chemical Sciences, Office of Basic Energy Sciences, Office of Energy Research, U.S. DOE.

REFERENCES

- [1] M. Drescher *et al.*, *Nature* **419**, 803 (2002).
- [2] L. Miaja-Avila *et al.*, *Phys. Rev. Lett.* **101**, 046101 (2008).
- [3] M. Schultze *et al.*, *Science* **328**, 1658 (2010).
- [4] A. L. Cavalieri *et al.*, *Nature* **449**, 1029 (2007); “Attosecond Time-Resolved Spectroscopy at Surfaces” in: *Dynamics at Solid State Surfaces and Interfaces, Vol. 1: Current development*, edited by U. Bovensiepen *et al.*, Wiley-VCH, Weinheim, 2010, pp. 537-553.
- [5] A. Kubo, K. Onda, H. Petek, Z. Sun, Y. S. Jung, and H. Koo Kim, *Nano Lett.* **5**, 1123 (2005).
- [6] M. Sukharev and T. Seideman, *Nano Lett.* **6**, 1123 (2006)
- [7] F. Le, N. Z. Lwin, N. J. Halas, and P. Nordlander *Phys. Rev. B* **76**, 165410 (2007).
- [8] M. I. Stockman, M. F. Kling, U. Kleineberg, and F. Krausz, *Nature Phot.* **1**, 539 (2007); M. I. Stockman, *Phys. Today* **64**, 39 (2011).
- [9] C.-H. Zhang and U. Thumm, *Phys. Rev. A* **82**, 043405 (2010).
- [10] S. Nagele, R. Pazourek, J. Feist, K. Doblhoff-Dier, C. Lemell, K. Tókési, and J. Burgdörfer, *J. Phys. B* **44**, 081001 (2011).
- [11] C.-H. Zhang and U. Thumm, *Phys. Rev. A* **84**, 033401 (2011).
- [12] A. S. Kheifets and I. A. Ivanov, *Phys. Rev. Lett.* **105**, 233002 (2010).
- [13] I. A. Ivanov, *Phys. Rev. A* **83**, 023421 (2011).
- [14] E. E. Krasovskii, *Phys. Rev. B* **84**, 195106 (2011).
- [15] C. Lemell, B. Solleder, K. Tókési, and J. Burgdörfer, *Phys. Rev. A* **79**, 062901 (2009).
- [16] A. K. Kazansky and P. M. Echenique, *Phys. Rev. Lett.* **102**, 177401 (2009).
- [17] C.-H. Zhang and U. Thumm, *Phys. Rev. Lett.* **102**, 123601 (2009); **103**, 239902(E) (2009).
- [18] C.-H. Zhang and U. Thumm, *Phys. Rev. A* **84**, 063403 (2011).
- [19] C.-H. Zhang and U. Thumm, *Phys. Rev. A* **84**, 065403 (2011).
- [20] C.-H. Zhang and U. Thumm, *Phys. Rev. A* **80**, 032902 (2009).
- [21] F. J. García de Abajo and P. M. Echenique, *Phys. Rev. B* **46**, 2663 (1992); **48**, 13399 (1993).
- [22] J. I. Gersten and N. Tzoar, *Phys. Rev. B* **8**, 5671 (1973); N. Tzoar and J. I. Gersten, *ibid.* **8**, 5684 (1973).